Journal of Magnetic Resonance 213 (2011) 26–31

Contents lists available at SciVerse ScienceDirect

Journal of Magnetic Resonance

journal homepage: www.elsevier.com/locate/jmr

A multi-frequency EPR spectroscopy approach in the detection of boson peak excitations

Marina Kveder [a,*], Dalibor Merunka [a], Amon Ilakovac [b], Boris Rakvin [a]

[a] Ruđer Bošković Institute, Bijenička 54, 10000 Zagreb, Croatia
[b] Faculty of Science, Bijenička 32, 10000 Zagreb, Croatia

ARTICLE INFO

Article history:
Received 21 June 2011
Revised 4 August 2011
Available online 31 August 2011

Keywords:
Boson peak
Multi-frequency EPR
Electron spin–lattice relaxation

ABSTRACT

The influence of boson peak (BP) excitations on low-temperature spin–lattice relaxation rate of a paramagnetic center embedded in a glassy matrix is investigated in the context of multi-frequency electron paramagnetic resonance (EPR) detection. In the theoretical analysis, the transition rate of spin one-half in the presence of a phonon field is calculated within the approximation of Fermi's golden rule. Several phonon densities of states are compared, among which one originating from a model of quasi-localized vibrations has been introduced into electron spin relaxation formalism for the first time. The respective frequency dependencies of spin–lattice relaxation rates are predicted which should lead to observable effects of BP modes if a multi-frequency study at very low temperatures is performed.

1. Introduction

One of the ubiquitous properties of almost all glasses is an excess in the vibrational density of states $\rho(\omega)$ over the prediction of the Debye theory [1]. This phenomenon shows up as a maximum in $\rho(\omega)/\omega^2$ and is termed the boson peak (BP) [2]. For different materials, the maximum densities of states at the peak appear in the range of frequencies between 0.4 and 2 THz [3]. The very nature of the BP is still extensively debated in the theory of condensed matter physics proposing specific theoretical models [4–7], while different experimental techniques have addressed the issue [8–11]. In this context, conventional *X*-band electron paramagnetic resonance (EPR) spectroscopy has presented very few results in which the impact of the BP has been discussed [3,12,13], the reason being that the EPR frequency only partially overlaps the BP frequency range. However, with advances in high frequency EPR spectrometers, the method is challenged to contribute toward the understanding of BP-related phenomena providing experimental data within the specific range of frequencies [14,15].

BP excitations are expected to play a role in electron spin –lattice relaxation, T_1, at low temperatures where phonon mechanisms dominate the energy exchange between the spin system and the lattice [16]. In this context, one-phonon processes are assumed to be the most important ones governing spin relaxation and exhibiting the linear temperature dependence of the respective $1/T_1$ data at the *X*-band EPR frequency [13,17]. These processes include several mechanisms, BP excitations being only one of them. Therefore, it is not possible to resolve the BP contribution by considering the temperature dependence of spin relaxation measurements performed at only one EPR frequency. For that reason, the aim of this study was to show how EPR spectroscopy performed at multiple frequencies and at low temperatures can contribute toward the detection of the BP contribution via frequency dependence of spin–lattice relaxation time measurements. Primary attention was focused on high-field EPR measurements, in which the resonant frequency approaches the BP maximum. It should be mentioned that lattice phonons can modulate different interactions, causing an energy exchange between the electron spin system and the lattice, which becomes frequency/magnetic-field dependent. For instance, in the direct or resonant process, the electron spin state is changed due to the absorption or emission of a resonant phonon, giving rise to $1/T_1^{\text{direct}} \propto \omega^2 T$ in the context of Debye theory [18]. When phonon modulation of *g* tensor anisotropy, Δg, is important, the frequency dependent electron spin–lattice relaxation rate should be additionally considered [19]. Phonon modulation of the electron spin–orbit coupling was extensively elaborated, showing that in the context of Debye model of phonon density of states, electron spin–lattice relaxation rates exhibit strong frequency dependence, $1/T_1^{\text{Kramers}} \propto \omega^4 T$ and $1/T_1^{\text{non-Kramers}} \propto \omega^2 T$ for Kramers and non-Kramers systems, respectively [16,20].

The analysis presented here is focused on the frequency/magnetic-field dependence of the electron spin–lattice relaxation rate, $1/T_1$, due to the BP excitations emerging from one-phonon mechanisms, such as the phonon modulation of electron-nuclear spin dipole–dipole coupling. Regarding multi-phonon processes, such

* Corresponding author.
E-mail address: kveder@irb.hr (M. Kveder).

1090-7807/$ - see front matter © 2011 Elsevier Inc. All rights reserved.
doi:10.1016/j.jmr.2011.08.029

as the Raman mechanism of spin relaxation when BP modes can be involved, this contribution should not be considered here because the Raman process cannot be resolved on the basis of respective frequency dependence and makes a minor contribution at low temperatures. In deriving $1/T_1$ formalism, the simplest approach was only intended to be considered as an initial approximation of the idea of a complex BP interrelation with electron-spin relaxation. It should be mentioned that the microscopic origin of BP phenomenon is still under dispute in terms of whether BP is related to the propagating plane waves and, thus, has a collective nature or is due to localized vibrational excitations. Since one of the first reports on the boson peak affecting electron spin–lattice relaxation was derived in the context of Debye formalism [3], the concept of our study was placed in the same framework. The following simplifications were assumed: (i) the involved spins are coupled via dipolar interaction while the lattice vibrations, in terms of the acoustic phonons, slightly displace their positions [21]; (ii) the transition probabilities between the initial and final states of the combined electron spin one-half and phonon system were calculated within the framework of Fermi's golden rule approximation; (iii) the validity of long-wave approximation within the normal coordinate expansion was anticipated.

In the context of this study, we emphasize that the frequency dependence of the spin–lattice relaxation rate is crucially determined by the assumed model of the phonon density of the states. Therefore, the densities of the phonon states according to Debye [22], modified Debye [3,19], for two-level tunneling systems (TLS) [23] and one developed within the model of quasi-localized vibrations (QLV) [24] were discussed. These were chosen due to their contributions regarding low temperature EPR experiments, except for the last one, which was introduced here for the first time into the field of EPR relaxation rate processes, although successfully applied in the analysis of the BP phenomena detected by other spectroscopic techniques [10]. We use the results of our study to propose the way how to make BP modes observable in the experimental data, if they participate in spin–lattice relaxation. In particular, we show that when BP excitations affect spin relaxation, a specific frequency dependence of $1/T_1$ should be experimentally derived, despite the universal temperature dependence of other one-phonon contributions. Therefore, we propose that high-field EPR spectroscopy, apart from being valuable in increasing the spectral resolution of overlapping paramagnetic species, can also contribute to the study of BP excitations and the development of a self-consistent description of the dynamical properties of glass-forming materials.

2. One-phonon processes and $1/T_1$

Following the text books on relaxation processes in magnetic resonance, the spin–lattice relaxation rate for a combined spin one-half and phonon system can be calculated by Fermi's golden rule approximation [16]

$$1/T_1 = w_{\alpha\beta} + w_{\beta\alpha}. \tag{1}$$

$w_{\alpha\beta}$ and $w_{\beta\alpha}$ denote transition probabilities/rates between the two spin one-half states α and β according to:

$$w_{\alpha\beta} = \frac{2\pi}{\hbar}\sum_{n'} |\langle\beta, n'|H|\alpha, n\rangle|^2 \delta(\hbar\omega - (E_\beta - E_\alpha)), \tag{2a}$$

$$w_{\beta\alpha} = \frac{2\pi}{\hbar}\sum_{n'} |\langle\alpha, n'|H|\beta, n\rangle|^2 \delta(\hbar\omega + (E_\alpha - E_\beta)). \tag{2b}$$

In the expression, H denotes the Hamiltonian, $E_{\alpha,\beta}$ are the respective energies related to the two involved spin states, n and n' refer to the phonon states and $\hbar\omega$ is the energy of the phonon that mediates the transition. The summation runs over the phonon states.

Here we focus on one-phonon processes that bring about the frequency/magnetic field dependence of electron spin relaxation, such as the phonon modulation of electron-nuclear spin dipolar interaction. In particular, electron–proton dipolar interaction is addressed explicitly while the extension to electron–electron coupling is straightforward.

Electron-nuclear spins coupled via dipolar interaction are exposed to lattice vibrations, which slightly displace their positions. For the purpose of simplicity, we explicitly consider only the fluctuations of the interspin distance due to the acoustic branch of the phonons (a more general approach is discussed in the Appendix A). The appropriate Hamiltonian can be approximated with

$$H = H_0 + H_{int}, \quad H_0 = H_Z + H_{ph}. \tag{3}$$

H_0 defines the combined spin-phonon states, with H_Z denoting the sum of single-spin Zeeman Hamiltonians in the absence of dipole coupling and H_{ph} is the lattice Hamiltonian. H_{int} is responsible for the phonon-mediated electron spin transitions in Eq. (2) characterized by the change in the electron magnetic quantum number $|\Delta m_i| = 1$. The relevant interaction Hamiltonian being the dipolar interaction between the electron spins i and proton spins j reads as follows in terms of [25]

$$H_{int} = -\sum_{ij}\frac{\gamma_S\gamma_N\hbar^2}{r_{ij}^3}(A + B + C), \tag{4a}$$

$$A = \frac{1}{4}(S^+I^- + S^-I^+)(1 - 3\cos^2\theta_{ij}), \tag{4b}$$

$$B = \frac{3}{2}\sin\theta_{ij}\cos\theta_{ij}(S^+I_Ze^{-i\varphi_{ij}} + S^-I_Ze^{+i\varphi_{ij}}), \tag{4c}$$

$$C = \frac{3}{4}\sin^2\theta_{ij}(S^+I^+e^{-2i\varphi_{ij}} + S^-I^-e^{+2i\varphi_{ij}}). \tag{4d}$$

r_{ij} denotes the distance between the coupled spins, θ_{ij} and φ_{ij} are the dipolar angles defining the orientation of the r_{ij}-vector with respect to the direction of the external magnetic field; γ_S and γ_I are electron and proton gyromagnetic rations while S^+, S^-, I^+, I^- and I_Z are electron and proton spin operators with their standard meanings, respectively [16].

The distance between the coupled spins can be expressed in terms of the respective rigid lattice distance, R_{ij}, and relative displacement, u_{ij}, due to the lattice vibrations

$$\vec{r}_{ij} = \vec{R}_{ij} + \vec{u}_{ij}, \quad \vec{R}_{ij} = \vec{R}_i - \vec{R}_j, \quad \vec{u}_{ij} = \vec{u}_i - \vec{u}_j. \tag{5}$$

Assuming that $|\vec{u}_{ij}| \ll |\vec{R}_{ij}|$, the expansion of $1/r_{ij}^3$ in Eq. (4) can be done up to the linear term and H_{int} factorized in the spin-dependent, h_S and phonon-dependent parts only, h_{ph}, as follows

$$H_{int} = \sum_{ij} h_S^{ij}(1 + h_{ph}^{ij}), \tag{6a}$$

with

$$h_S^{ij} = -\frac{\gamma_S\gamma_N\hbar^2}{R_{ij}^3}(A + B + C), \tag{6b}$$

and

$$h_{ph}^{ij} = -3\frac{(\vec{u}_i - \vec{u}_j)\vec{R}_{ij}}{R_{ij}^2}. \tag{6c}$$

In the context of this study, the matrix elements involving H_{int} with h_{ph}^{ij} are the focus of interest as they give rise to the temperature and frequency dependence of the spin–lattice relaxation rate. The displacement vector can be expressed by making use of normal coordinate expansion

$$\vec{u}_i = \sum_{\vec{k},s} \sqrt{\frac{\hbar}{2MN\omega_{\vec{k}}}} \vec{e}_{\vec{k}} e^{i\vec{k}\vec{R}_i} (a_{\vec{k}} + a^{+}_{-\vec{k}}), \tag{7}$$

with $\vec{k}$ denoting phonon wave vector, N is the number of normal modes bearing the polarization vector, $\vec{e}_{\vec{k}}$, s denotes polarization index, M is the ionic mass while $a^{+}_{\vec{k}}$ and $a_{-\vec{k}}$ are phonon creation and annihilation operators [22]. Assuming long-wave approximation, the relative displacement reads

$$\vec{u}_i - \vec{u}_j = \sum_{\vec{k},s} \sqrt{\frac{\hbar}{2MN\omega_{\vec{k}}}} \vec{e}_{\vec{k}} ikR_{ij} \cos\phi_{ij} e^{i\vec{k}\vec{R}_j} (a_{\vec{k}} + a^{+}_{-\vec{k}}) \tag{8}$$

where ϕ_{ij} refers to the angle between $\vec{R}_{ij}$ and $\vec{k}$. In order to calculate h^{ij}_{ph}, the contributions of both the longitudinal (L) and transverse (T) phonon polarizations are taken into account. Combining Eq. (8) with Eq. (6c) and realizing that only one out of two transverse polarizations makes a contribution, the following expression is obtained

$$h^{ij}_{ph} = -3i\left(\sum_{\vec{k}} \sqrt{\frac{\hbar\omega^{L}_{\vec{k}}}{2MNc^{2}_{L}}} \cos^2\phi_{ij} e^{i\vec{k}\vec{R}_j} \left(a_{\vec{k}} + a^{+}_{-\vec{k}}\right)_L + \sum_{\vec{k}} \sqrt{\frac{\hbar\omega^{T}_{\vec{k}}}{2MNc^{2}_{T}}} \cos\phi_{ij} \sin\phi_{ij} e^{i\vec{k}\vec{R}_j} \left(a_{\vec{k}} + a^{+}_{-\vec{k}}\right)_T \right). \tag{9}$$

By taking into account Eq. (9), which defines one-phonon-mediated spin transitions, the transition probabilities defined in Eq. (2) for an electron–proton spin pair coupled by dipolar interaction read

$$w^{ij}_{\alpha\beta} = \frac{2\pi}{\hbar} 9 \sum_n A^{ij} \left(\cos^4\phi_{ij} \frac{\hbar\omega^{L}_{\vec{k}}}{2MNc^{2}_{L}} n^{L}_{\vec{k}} \delta\left(\hbar\omega^{L}_{\vec{k}} - (E_\beta - E_\alpha)\right) + \cos^2\phi_{ij} \sin^2\phi_{ij} \frac{\hbar\omega^{T}_{\vec{k}}}{2MNc^{2}_{T}} n^{T}_{\vec{k}} \delta\left(\hbar\omega^{T}_{\vec{k}} - (E_\beta - E_\alpha)\right) \right), \tag{10a}$$

$$w^{ij}_{\beta\alpha} = \frac{2\pi}{\hbar} 9 \sum_n A^{ij} \left(\cos^4\phi_{ij} \frac{\hbar\omega^{L}_{\vec{k}}}{2MNc^{2}_{L}} (n^{L}_{\vec{k}} + 1) \delta\left(\hbar\omega^{L}_{\vec{k}} + (E_\alpha - E_\beta)\right) + \cos^2\phi_{ij} \sin^2\phi_{ij} \frac{\hbar\omega^{T}_{\vec{k}}}{2MNc^{2}_{T}} (n^{T}_{\vec{k}} + 1) \delta\left(\hbar\omega^{T}_{\vec{k}} + (E_\alpha - E_\beta)\right) \right). \tag{10b}$$

A^{ij} contains spin-dependent parts, including the spatial orientation between the coupled spins, and $n_{\vec{k}}$ denotes the mean number of phonons with wave vector $\vec{k}$ and energy $\hbar\omega_{\vec{k}}$ that are present at temperature T

$$n_{\vec{k}} = \frac{1}{e^{(\hbar\omega_{\vec{k}}/k_B T)} - 1}.$$

k_B denotes the Boltzmann constant. The summation over the phonon states can be replaced by a summation over the directions of the wave vectors $\vec{k}$ and over the phonon frequencies [21]. In particular, the isotropic distribution of the wave vector directions can be assumed as giving rise to the factors 1/5 for longitudinal and 2/15 for the transverse polarizations of the phonons, while the summation over phonon frequencies can be replaced by an integration over the phonon density of the states. Therefore, within the approximations used in the calculations, the difference in the phonon polarization states does not affect the frequency dependence of the spin–lattice relaxation rate, the primary subject of this study. Including the summation over the spin pairs coupled by dipolar interaction, Eq. (1) finally reads

$$1/T_1 = B\rho(\omega_{EPR})\omega_{EPR} \coth\left(\frac{1}{2}\frac{\hbar\omega_{EPR}}{k_B T}\right). \tag{11}$$

B contains, apart from the spin-dependent terms, all the numerical factors and $\rho(\omega_{EPR})$ is the phonon density of states at the working EPR frequency, $\omega_{EPR} = |E_\beta - E_\alpha|/\hbar$. Inspection of Eq. (11) indicates that the frequency dependence of the spin–lattice relaxation rate is crucially determined by the assumed model of $\rho(\omega_{EPR})$. Therefore, we discuss models of $\rho(\omega_{EPR})$ related to boson peak excitations in the context of multi-frequency low-temperature $1/T_1$ measurements.

3. Discussion

In this study, we focus on one-phonon mechanisms that bring about a specific frequency/magnetic field dependence of electron spin relaxation due to the involvement of boson peak effects. The analysis relies on Eq. (11), essentially representing a two-dimensional problem in which the microwave frequency and temperature dependence should be disentangled. The information about the BP effect is operatively contained in the former property while the latter depends on the hyperbolic cotangent function, which exhibits two interesting limits at low temperatures(1–15 K). When spin–lattice relaxation rates are determined at frequencies lower than the Q-band EPR (34 GHz), only the first term of the Taylor expansion in the hyperbolic cotangent function can be taken into account due to $k_B T \ll \hbar\omega_{EPR}$, thus, rendering $1/T_1 \propto T$. On the other hand, at higher EPR frequencies above W-band EPR (94 GHz), the hyperbolic cotangent function approaches unity due to $k_B T \ll \hbar\omega_{EPR}$. This is illustrated in Fig. 1. It can clearly be seen that by increasing the EPR frequency from the X-band (10 GHz) to higher frequencies, the temperature dependence of $1/T_1$ levels off below 10 K. For instance, the hyperbolic cotangent function evaluated at 5 K reads 1.2, 1.04, and 1 for the EPR frequencies of 263 GHz, 400 GHz and 700 GHz, respectively. This means that above 263 GHz, according to the formalism presented by Eq. (11), any relaxation mechanism including terms such as given in Eq. (4) would experimentally sample temperature independent $1/T_1$ at $T \leqslant 5$ K. This phenomenon points to a practical experimental consequence, i.e., the higher the frequency, the broader the low-temperature interval where the acquired data are not expected to depend on the temperature due to the hyperbolic cotangent function term (e.g., this condition is already fullfilled at 10 K for experiments performed at 700 GHz). Fulfilling this condition according to Eq. (11), $1/T_1$ becomes solely frequency dependent and in principle makes it possible to verify the involvement of BP excitations in the energy exchange between the electron spin and the lattice by performing measurements at several high frequencies/magnetic fields. Following this reasoning, we discuss the frequency dependence of $1/T_1$ behavior predicted from various models of the phonon density of states assuming temperature-independent $1/T_1$.

3.1. Modified Debye model

One of the first reports on the boson peak affecting electron spin–lattice relaxation in amorphous materials in the context of one-phonon relaxation mechanisms proposed a modified Debye density of states [3]

$$\rho(\omega) = \frac{9N\omega^2}{\omega_D^3}\left[1 + \mu\frac{\omega^2_{BP}}{\omega^2} e^{-\left(\ln(\omega/\omega_{BP})/(\sqrt{2}\sigma)\right)^2}\right], \tag{12}$$

with N denoting the total number of acoustic phonon modes, ω_D being the Debye frequency, and μ and σ being constants in the range of 2–10 and 0.48, respectively. The first term in Eq. (12) corresponds to the phonon density of states according to the standard Debye model [22], while the second term describes the contribution of vibrational excitations in the vicinity of ω_{BP} characterized by the width, σ, of the boson peak distribution. Substituting Eq. (12) into Eq. (11), the spin–lattice relaxation rate reads

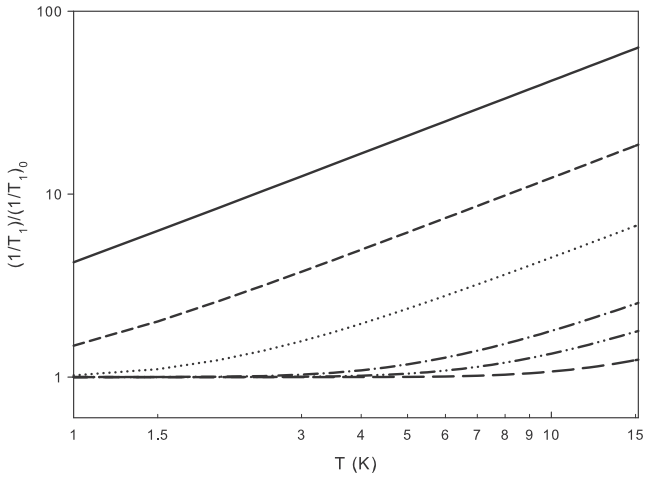

Fig. 1. Temperature dependence of spin–lattice relaxation rate, $1/T_1$, according to Eq. (11) presented for the following frequencies: *X*-band (solid line), *Q*-band (short dash line), *W*-band (dotted line), 250 GHz (dash-dot line), 400 GHz (dash-dot-dot line) and 700 GHz (long dash line). Data are expressed in terms of spin–lattice relaxation rate at $T = 0$ K, $(1/T_1)_0$.

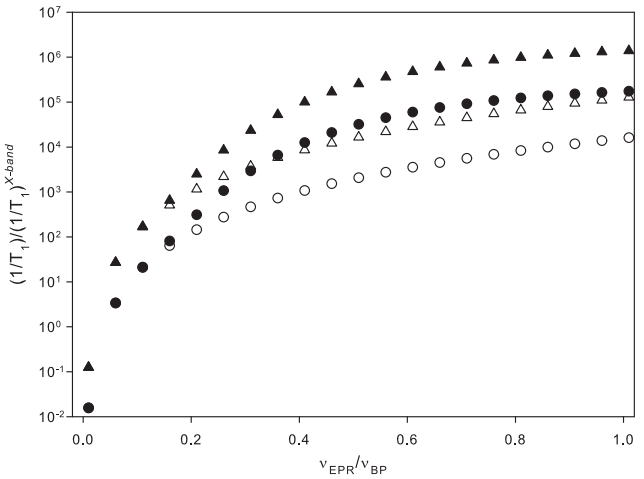

Fig. 2. Frequency dependence of spin–lattice relaxation rate, $1/T_1$, calculated for $T = 0$ K according to the modified Debye model [3,19] given in Eq. (13) assuming $\mu = 10$, $\sigma = 0.48$, (full symbols). The comparison is made with respect to the Debye model (empty symbols) for two boson peak frequencies: $\nu_{BP} = 500$ GHz (triangles) and $\nu_{BP} = 250$ GHz (circles). Data are expressed in terms of spin–lattice relaxation rates at *X*-band frequency, $(1/T_1)^{X\text{-band}}$, in order to eliminate all the constants from the expression.

$$1/T_1 \propto \frac{\omega_{EPR}^3}{\omega_D^3}\left[1+\mu\frac{\omega_{BP}^2}{\omega_{EPR}^2}e^{-(\ln(\omega_{EPR}/\omega_{BP})/(\sqrt{2}\sigma))^2}\right]\coth\left(\frac{1}{2}\frac{\hbar\omega_{EPR}}{k_BT}\right). \quad (13)$$

The expected frequency dependence of the spin–lattice relaxation rate is shown in Fig. 2 and compared with the Debye model. It should be noted that in this approach, the BP contribution is positioned at will at a certain EPR frequency, where it causes a small "hump" in the otherwise monotonous increase of $1/T_1$, with an increase in EPR frequency as predicted by the Debye theory.

3.2. Model of quasi-localized vibrations

The thermal properties of glasses at low frequencies, $\omega \ll \omega_D$, and low temperatures, $T \ll T_D$, have usually been discussed in the standard model of non-interacting two-level systems (TLS), which exist in glass but not in crystal [26]. In this concept, the motion of nuclei within the TLS double-well potential provokes time-dependent perturbation of the nearby electron spins via electron-nuclear dipolar interaction [23]. From the two processes involved in TLS dynamics, tunneling and thermally activated processes, only the former should be taken into account when low temperature one-phonon-assisted tunneling is involved. Assuming that the tunneling mode energies are below the thermal energy, the electron spin–lattice relaxation rate can be expressed as [23]

$$1/T_1 \propto \frac{1}{\omega_{EPR}^2}T. \quad (14)$$

This approach predicts that longer T_1 will be sampled with an increase in the experimental frequency in a glassy sample, which is completely different behavior from that expected from the Debye theory describing the crystalline state of matter.

On the other hand, the boson peak, as a universal property of glasses, is observed at much higher frequencies and, thus, is usually considered separately from the TLS [11]. However, in the model of quasi-localized vibrations (QLV), a physical picture has been presented in which the interrelation of the TLS and boson peak excitations was proposed [24]. This approach was successfully applied in the analysis of fluorescent single-molecule spectroscopic data [10], subterahertz hypersound attenuation measurements [27] and neutron scattering data [28]. Essentially, the QLV model evolved from the "soft-mode" model [29,30], which postulated that in glassy systems the participation of both harmonic (Debye phonons) and anharmonic dynamics at temperatures far below the liquid-glass transition should be considered [31,32]. The idea was further elaborated within the QLV model, which focuses on quasi-localized harmonic modes, understood as local low-frequency vibrations, undergoing weak interactions with the high frequency surroundings (e.g., sound waves) and with each other [24]. Due to this interaction between soft and high-frequency oscillators, vibrational instability occurs that is controlled by the anharmonicity, similarly to bilinearly coupled harmonic oscillators that become unstable when the respective interaction exceeds a critical value [33]. Due to the same mechanism of vibrational instability, the vibrational density of the states of low-frequency harmonic oscillators is reconstructed in such a way that two-level systems are created simultaneously with the boson peak. These collective low-frequency vibrations exhibit the density of vibrational states [24]

$$\rho(\omega) = C\frac{\omega^4}{\omega_*^3}\int_0^{\sqrt{3/2}}\frac{dt}{1+\left(\frac{\omega}{\omega_*}\right)^6 t^2(3-2t^2)^2}, \quad (15)$$

where C includes all the constant terms and it is assumed that $\omega_* \approx \omega_{BP}$. The boson peak at $\omega \approx \omega_{BP}$ corresponds to the maximum in the reduced density of states, $\rho(\omega)/\omega^2$, when plotted against ω/ω_*.

In the framework of the QLV model, here we present for the first time a prediction of the electron spin–lattice relaxation rate related to the detection of the boson peak by EPR spectroscopy. However, it should be mentioned that within the simplified concept of BP excitations affecting electron spin relaxation presented in this study, the rationale for combining the parameters from the QLV model with the essentially collective nature of the formalism defining $1/T_1$ is due to the fact that the soft-modes are not the exact eigenstates of the glass because they are mixed with acoustic phonons [33] and 10–100 atoms can be involved in the vibrational displacement [34]. Introducing the QLV density of the states from Eq. (15) into the expression for the electron spin–lattice relaxation rate, Eq. (11) reads

$$1/T_1 \propto x^5\int_0^{\sqrt{3/2}}\frac{dt}{1+x^6t^2(3-2t^2)^2}\coth\frac{1}{2}\frac{x}{k_BT}\hbar\omega_{BP},\ x=\frac{\omega_{EPR}}{\omega_{BP}}. \quad (16)$$

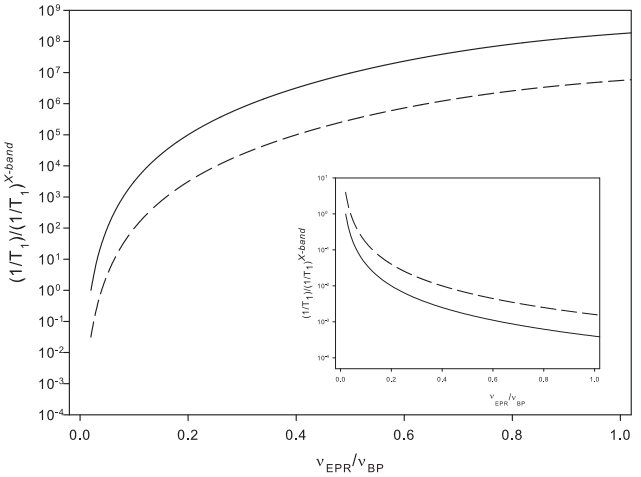

Fig. 3. Prediction of the frequency dependence of spin–lattice relaxation rate, $1/T_1$, calculated for $T = 0$ K according to QLV model [24] given in Eq. (16) assuming $\nu_{BP} = 500$ GHz (full line) and $\nu_{BP} = 250$ GHz (dashed line). In the inset to the figure, the prediction according to Eq. (14) in the context of TLS excitations is provided [23]. Data are expressed in terms of spin–lattice relaxation rates at *X*-band frequency, $(1/T_1)^{X\text{-}band}$, in order to eliminate all the constants from the expression.

It can be shown that the integral in Eq. (16) is constant up to $\omega_{EPR} \approx 0.8\omega_{BP}$. In this case, the spin–lattice relaxation rate is scaled with a frequency to the power of 5 when the hyperbolic cotangent function is close to unity or to the power of 4 when $k_B T \gg \hbar\omega_{EPR}$. The frequency dependence of $1/T_1$ according to Eq. (16) is presented (Fig. 3).

In conformity with the preceding analysis, checking for BP involvement in the experimental relaxation rate data should be strongly considered when a shorter T_1 sampling with an increase in the experimental frequency, as compared to the Debye frequency behavior, is detected at low temperatures. According to the presented formalism, strong frequency dependence is to be expected in the multi-frequency analysis of $1/T_1$. In this case, an enhanced energy exchange between the spin system and the lattice in the glassy systems can be anticipated due to the BP excitations.

4. Conclusion

The analysis presented here was motivated by sparse low temperature $1/T_1$ data measured at several EPR frequencies [35–38]. In addition, the impact of the BP had previously been rarely discussed in the context of electron spin coupling with the lattice [3,13]. Therefore, the aim was to show that a multi-frequency EPR approach can be exploited to disentangle BP involvement in electron spin relaxation in glassy solids at temperatures below ca. 10 K. The sensitivity of the approach relies on the distinct frequency dependence of $1/T_1$ in glassy versus crystalline solids. The predictions derived within the models of the phonon density of states point to the greater dependence of $1/T_1$ on EPR frequencies as compared to the predictions of the standard Debye model, what should make BP experimentally discernable. In particular, the expected shorter T_1 sampling with an increase in the experimental frequency should clearly rule out the mechanism involving TLS excitations. The verification of the exact theoretical model is left to the adequate multi-frequency/high magnetic field EPR study.

Acknowledgment

This study was supported by the Croatian Ministry of Science, Education and Sports, Grants Nos. 098-0982915-2939 and 119-0982930-1016.

Appendix A

Considering the interaction Hamiltonian presented in Eq. (6) in the analysis of the phonon-dependent electron $1/T_1$, one should generally take into account both the fluctuations of the interspin distance, $r_{ij} = R_{ij} + \Delta r_{ij}$, and dipolar angle, $\theta_{ij} = \Theta_{ij} + \Delta\theta_{ij}$, according to

$$H_{int} = \sum_{ij} H_{int}(r_{ij}, \theta_{ij}) = -\sum_{ij} \frac{\gamma_S \gamma_N \hbar^2}{r_{ij}^3} \left(A(\Theta_{ij} + \Delta\theta_{ij}) + B(\Theta_{ij} + \Delta\theta_{ij}) + C(\Theta_{ij} + \Delta\theta_{ij})\right). \tag{1A}$$

The series expansion of Eq. (1A) up to the linear term in u reads

$$H_{int} = \sum_{ij} H_{int} + \Delta u_{II}^{ij} \left[\frac{\partial H_{int}}{\partial r_{ij}}\right]_{r_{ij}=R_{ij}} + \Delta u_{\perp}^{ij} \left[\frac{1}{R_{ij}} \frac{\partial H_{int}}{\partial \theta_{ij}}\right]_{\theta_{ij}=\Theta_{ij}}, \tag{2A}$$

with

$$\Delta r_{ij} = \Delta u_{II}^{ij} = (\vec{u}_i - \vec{u}_j)\vec{R}_{ij}/R_{ij} \text{ and } \Delta\theta_{ij} = \Delta u_{\perp}^{ij}/R_{ij}. \tag{2B}$$

As shown by Eq. (9)

$$\Delta u_{II}^{ij} = |\vec{u}_i - \vec{u}_j| \cos\phi_{ij} \text{ and } \Delta u_{II}^{ij} = |\vec{u}_i - \vec{u}_j| \sin\phi_{ij}, \tag{3A}$$

for longitudinal and transverse acoustic phonons, respectively. We illustrate the effect of dipolar angle fluctuations by assuming that $\vec{k}$, $\vec{R}_{ij}$ and the magnetic field vector are coplanar. In that case, one obtains

$$\Delta u_{\perp}^{ij} = |\vec{u}_i - \vec{u}_j| \sin\phi_{ij} \text{ and } \Delta u_{\perp}^{ij} = |\vec{u}_i - \vec{u}_j| \cos\phi_{ij}, \tag{3B}$$

for longitudinal and transverse acoustic phonons, respectively. It should be pointed out that, with respect to this very special case, the general orientation of $\vec{k}$, $\vec{R}_{ij}$ and the magnetic field vector would bring, apart from different angular terms, the same linear dependence on the atomic displacement that is the main subject of this study. Therefore, we can conclude that since both the angular and distance fluctuations depend linearly on the atomic displacement, the same type of frequency dependence of the electron $1/T_1$ will be induced. In particular, the main result of this investigation focused on the frequency dependence of the electron $1/T_1$, derived solely by explicitly considering the fluctuations of the interspin distance within the presented formalism, is of general value. A similar conclusion regarding the temperature dependence of phonon-assisted spin diffusion rates in solids was reported for NMR [21].

References

[1] R. Zorn, Boson peak in confined disoredered systems, Physical Review B 81 (2010) 054208.
[2] S.A. Abraham, B. Bagchi, Vibrational dynamics and boson peak in a supercooled polydisperse liquid, Physical Review E 81 (2010) 031506.
[3] N.P. Giorgadze, L.Zh. Zakharov, Effect of boson peak on low-temperature electron spin-lattice relaxation in amorphous materials, Low Temperature Physics 24 (1998) 198–200.
[4] T.S. Grigera, V. Martin-Mayor, G. Parisi, P. Verrocchio, Phonon interpretation of the "boson peak" in supercooled liquids, Nature 422 (2003) 289–292.
[5] W. Schirmacher, Thermal conductivity of glassy materials and the "boson peak", Europhysics Letters 73 (2006) 892–898.
[6] H. Shintani, H. Tanaka, Universal link between the boson peak and transverse phonons in glass, Nature Materials 7 (2008) 870–877.
[7] H.M. Flores-Ruiz, G.G. Naumis, Boson peak as a consequence of rigidity: a perturbation theory approach, Physical Review B 83 (2011) 184204.
[8] M.A. Ramos, S. Vieira, F.J. Bermejo, J. Dawidowski, H.E. Fischer, H. Schober, M.A. González, C.K. Loong, D.L. Price, Quantitative assessment of the effects of orientational and positional disorder on glassy dynamics, Physical Review Letters 78 (1997) 82–85.
[9] H. Leyser, W. Doster, M. Diehl, Far-infrared emission by boson peak vibrations in a globular protein, Physical Review Letters 82 (1999) 2987–2990.

[10] Yu.G. Vainer, A.V. Naumov, L. Kador, Local vibrations in disordered solids studied via single-molecule spectroscopy: comparison with neutron, nuclear, Raman scattering, and photon echo data, Physical Review B 77 (2008) 224202.
[11] B. Ruta, G. Baldi, V.M. Giordano, L. Orsingher, S. Rols, F. Scarponi, G. Monaco, Communication: high-frequency acoustic excitations and boson peak in glasses: a study of their temperature dependence, Journal of Chemical Physics 133 (2010) 041101.
[12] B. Rakvin, N. Maltar-Strmečki, C.M. Ramsey, N.S. Dalal, Heat capacity and electron spin echo evidence for low frequency vibrational modes and lattice disorder in L-alanine at cryogenic temperatures, Journal of Chemical Physics 120 (2004) 6665–6673.
[13] M. Kveder, D. Merunka, M. Jokić, J. Makarević, B. Rakvin, Electron spin-lattice relaxation in solid ethanol: effect of nitroxyl radical hydrogen bonding and matrix disorder, Physical Review B 80 (2009) 052201.
[14] J. Wang, Z. Wang, R.J. Clark, A. Ozqrowski, J. van Tol, N.S. Dalal, A High-field EPR characterization of the $S = 2$ linear Tri-atomic chain in Cr_3 $(dpa)_4$ $Cl_2CH_2Cl_2$, Polyhedron (2011), doi:10.1016/j.poly.2011.02.032.
[15] T. Sakurai, T. Horie, M. Tomoo, K. Kondo, N. Matsumi, S. Okubo, H. Ohta, Y. Uwatoko, K. Kudo, Y. Koike, H. Tanaka, Development of high-pressure, high-field and multi-frequency ESR apparatus and its application to quantum spin system, Journal of Physics: Conference Series 215 (2010) 012184.
[16] A. Abragam, B. Bleaney, Electron Paramagnetic Resonance of Transition Ions, Oxford University Press, Oxford, 1970. p. 551.
[17] V. Kathirvelu, H. Sato, S.S. Eaton, G.R. Eaton, Electron spin relaxation rates for semiquinones between 25 and 295 K in glass-forming solvents, Journal of Magnetic Resonance 198 (2009) 111–120.
[18] M.K. Bowman, L. Kevan, Electron spin-lattice relaxation in nonionic solids, in: L. Kevan, R.N. Schwartz (Eds.), Time Domain Electron Spin Resonance, John Wiley & Sons, Inc., 1979, p. 82.
[19] L.G. Zakharov, L.L. Chotorlishvili, T.L. Buishvili, Two-quantum electron spin-lattice relaxation in amorphous solids, Low Temperature Physics 28 (2002) 412–414.
[20] R. Orbach, Spin-lattice relaxation in rare-earth salts, Proceedings of the Royal Society of London A 264 (1961) 458–484.
[21] J. Dolinšek, P.M. Cereghetti, R. Kind, Phonon-assisted spin diffusion in solids, Journal of Magnetic Resonance 146 (2000) 335–344.
[22] C. Kittel, Introduction to Solid State Physics, John Wiley & Sons, Inc., 1996. p. 122.
[23] M.K. Bowman, L. Kevan, An electron spin-lattice relaxation mechanism involving tunneling modes for trapped radicals in glassy matrices. Theoretical development and application to trapped electrons in γ-irradiated ethanol glass, Journal of Physical Chemistry 81 (1977) 456–462.
[24] D.A. Parshin, H.R. Schober, V.L. Gurevich, Vibrational instability, two-level systems, and the boson peak in glasses, Physical Review B 76 (2007) 064206.
[25] C.P. Slichter, Principles of Magnetic Resonance, Springer-Verlag, 1996. p. 66.
[26] S.R. Kurtz, H.J. Stapleton, Effects of disorder on electron-spin relaxation in β-alumina: a prototype glass, Physical Review B 22 (1980) 2195–2205.
[27] S. Ayrinhac, M. Foret, A. Devos, B. Rufflé, E. Courtens, R. Vacher, Subterahertz hypersound attenuation in silica glass studied via picoseconds acoustics, Physical Review B 83 (2011) 014204.
[28] B. Rufflé, D.A. Parshin, E. Courtens, R. Vacher, Boson peak and its relation to acoustic attenuation in glasses, Physical Review Letters 100 (2008) 015501.
[29] V.G. Karpov, M.I. Klinger, P.N. Ignatiev, Atomic tunneling states and low-temperature anomalies of thermal properties in amorphous materials, Solid State Communication 44 (1982) 333–337.
[30] D.A. Parshin, Soft potential model and universal properties of glasses, Physica Scritpa T49 (1993) 180–185.
[31] H.R. Schober, D.A. Parshin, V.L. Gurevich, Quasi-localized vibrations, boson peak and tunneling in glasses, Journal of Physics: Conference Series 92 (2007) 012131.
[32] M.I. Klinger, Soft atomic motion modes in glasses: their role in anomalous properties, Physics Reports 492 (2010) 111–180.
[33] U. Buchenau, Yu.M. Galperin, V.L. Gurevich, D.A. Parshin, M.A. Ramos, H.R. Schober, Interaction of soft modes and sound waves in glasses, Physical Review B 46 (1992) 2798–2808.
[34] U. Buchenau, Yu.M. Galperin, V.L. Gurevich, H.R. Schober, Anharmonic potentials and vibrational localization in glasses, Physical Review B 43 (1991) 5039–5045.
[35] S.S. Eaton, J. Harbridge, G.A. Rinard, G.R. Eaton, R.T. Weber, Frequency dependence of electron spin relaxation for three $S = ½$ species doped into diamagnetic hosts, Applied Magnetic Resonance 20 (2001) 151–157.
[36] J.S. Hyde, Jun-Jie Yin, W.K. Subczynski, T.G. Camenisch, J.J. Ratke, W. Froncisz, Spin-label EPR T_1 values using saturation recovery from 2 to 35 GHz, Journal of Physical Chemistry B 108 (2004) 9524–9529.
[37] H. Sato, V. Kathirvelu, G. Spagnol, S. Rajca, A. Rajca, S.S. Eaton, G.R. Eaton, Impact of electron–electron spin interaction on electron spin relaxation of nitroxide diradicals and tetraradical in glassy solvents between 10 and 300 K, Journal of Physical Chemistry B 112 (2008) 2818–2828.
[38] W. Froncisz, T.G. Camenisch, J.J. Ratke, J.R. Anderson, W.K. Subczynski, R.A. Strangeway, J.W. Sidabras, J.S. Hyde, Saturation recovery EPR and ELDOR at *W*-band for spin labels, Journal of Magnetic Resonance 193 (2008) 297–304.